INDIAN JOURNAL OF SCIENCE AND TECHNOLOGY

RESEARCH ARTICLE

Experimental Investigation of Supersonic Jet Control Using Sonic Air Tabs

G Mahendra Perumal[1,2], S M Aravindh Kumar[1]*, S Elangovan[2], M Sundararaj[2]

1 Department of Aerospace Engineering, SRM Institute of Science and Technology, Kattankulathur, Chennai, 603203, India
2 Department of Aeronautical Engineering, Bharath Institute of Higher Education and Research, Selaiyur, Chennai, 600126, India

OPEN ACCESS

Received: 31-07-2023
Accepted: 09-09-2023
Published: 22-10-2023

Citation: Perumal GM, Aravindh Kumar SM, Elangovan S, Sundararaj M (2023) Experimental Investigation of Supersonic Jet Control Using Sonic Air Tabs. Indian Journal of Science and Technology 16(39): 3343-3352. https://doi.org/10.17485/IJST/v16i39.1918

* **Corresponding author**.

aravindm1@srmist.edu.in

Funding: None

Competing Interests: None

Published By Indian Society for Education and Environment (iSee)

ISSN
Print: 0974-6846
Electronic: 0974-5645

Abstract

Objectives: The primary objective of the study is to understand the influence of two sonic air tabs on the mixing characteristics of a supersonic (Mach 2.1) circular jet. **Methods:** In the high-speed open jet facility, a convergent-divergent nozzle delivering Mach 2.1 jet was controlled using two air tabs positioned at the nozzle exit. The injection pressure ratio of the air tabs varied from 3 to 6 for a nozzle pressure ratio of 3, 4, 5, and 6. Pitot pressure measurements and flow visualization were performed for controlled and uncontrolled jets. **Findings:** The results of the pitot pressure measurements showed a significant decrease in core length for the nozzle pressure ratios investigated. The core length reduction was attributed to the accelerated mixing of the Mach 2.1 jet with the surrounding fluid due to the air tabs. Furthermore, with the increase in the injection pressure ratio, the mixing enhancement due to the air tabs was observed to be increasing. The maximum reduction in core length occurred at an injection pressure ratio of 6 resulting in reductions of 86.1%, 64.9%, 61.1%, and 56.4% for nozzle pressure ratios 3, 4, 5, and 6, respectively. The visualization results confirmed the efficiency of the air tabs' in decreasing the strength of waves in the jet core region. **Novelty:** The novelty of this study lies in the use of two sonic air tabs for controlling supersonic jets. Unlike other control techniques, these air tabs can be activated or deactivated as needed without compromising the overall aircraft performance.

Keywords: Air Tab; Supersonic Jet; Injection Pressure Ratio; Nozzle Pressure Ratio; Shadowgraph

1 Introduction

Any aerospace vehicle needs an efficient propulsion system to function smoothly across different regimes. In propulsion systems, thrust is generated when gas at high pressure expands through a nozzle, resulting in high-velocity jets. Research on jet control focuses on thrust augmentation and thrust vectoring. The mechanical means of thrust vectoring focus on the use of solid grooves, notches, nozzles, tabs, swirls, and chevrons. These

structures generate counter-rotating vortices against the normal jet flow, promoting efficient jet mixing[1,2]. Several studies have explored the use of tabs of various shapes for controlling high-speed jets. Solid tabs are preferred owing to their simple geometry and improved mixing enhancement compared to other techniques[3]. In the case of an over-expanded nozzle, the flow generates shock waves, resulting in unsteady boundary layer parting. Within the expansion system of the nozzles, various complex physical phenomena like supersonic jets, adverse pressure gradients, shock waves, and jet separation can significantly affect the overall performance[4].

A more efficient method of thrust vectoring, known as fluidic thrust control or secondary injection, has emerged as a promising jet control strategy following Davis's study in 1982. At the nozzle exit of a Mach 0.8 jet, two steady injectors spaced 180 degrees apart were used to produce jet mixing[5]. Over the past 50 years, fluidic injection has been investigated for reducing jet noise sources and modifying jet velocity and temperature profiles. Fluidic injection improves mixing in the shear layer that separates the jet plume from its surroundings and provides performance flexibility by enabling a change in the regulating parameters. Unlike other control techniques, fluidic injection provides thrust augmentation with mixing enhancement, and the injectors can be activated or deactivated as needed without affecting overall aircraft performance. Fluidic injectors can also be used for thrust vector control, noise reduction, and drag reduction. Fluidic injection control has made a significant contribution to lowering vehicle weight, lowering maintenance needs, and improving the stealthiness of aircraft, rockets, and missiles[1,5]. The current investigation focuses on the impact of fluidic injection in sonic air tab-based supersonic jet systems.

"Injection Pressure Ratio (IPR) is termed the ratio of the stagnation/supply pressure of the secondary jet to the freestream stagnation pressure"[1]. The impact of IPR on the flow properties of a supersonic main jet flow has been an important aspect of research. In the Mach 1.56 jet, the mixing efficiency and the angle of fluidic injection were investigated by Semlitsch and Mihaescu[6]. The injectors were evenly distributed at the nozzle exit, with injector numbers (N) of 6, 12, and 24. The findings indicated that steeper injection angles resulted in enhanced jet mixing in comparison to shallower injection angles. According to Perumal and Zhou's study[7] on the impact of injector number (N) on the mixing properties of a subsonic jet, the rate of jet decay decreases as N grows for a certain injector diameter to nozzle diameter (d/D) ratio. The scaling analysis of a Mach 2.0 jet was reported by Arun Kumar et al.[5] results showed that reducing the nozzle pressure ratio leads to a decrease in the ratio of injection pressure to main jet pressure, and cutting the injection width in half increases control effectiveness. Sekar et al.[8] have studied the performance of a converging nozzle with fluid thrust vectoring using secondary jet injection. They reported that the thrust coefficient was dependent on the nozzle pressure ratio (NPR) and mass ratio, while the vector angle was only dependent on the mass ratio, and the secondary injection increased the magnitude of the net thrust while reducing the thrust coefficient.

In a supersonic jet, the axial velocity does not remain uniform within the core region, as observed in subsonic jets. Rather, the core region of the supersonic jet experiences a series of shockwaves and expansion waves. The supersonic jet core can be defined as the axial distance span from the nozzle outlet to the point where the characteristic velocity changes begin, or the location along the axis where the influence of waves from the nozzle outlet remains dominant[9].

Previous works have studied the effect of solid tabs, chevrons, nozzles, etc. on jet control. The present study is novel in using sonic air tabs in a supersonic (Mach 2.1) jet system. To mimic the effects of solid tabs, a fluidic injector comprising two small control jets injecting air radially into the main jet was used. The major objective of the experiment was to understand the impact of air tabs on a supersonic jet (Mach 2.1) positioned at the nozzle exit while varying the IPR from 3 to 6 and maintaining a fixed NPR of 3, 4, 5, and 6. The core length assessment of the supersonic jet was conducted between configurations with and without air tabs. This analysis involved studying pitot pressure measurements and examining corresponding shadowgraph images of the jets under controlled experimental conditions.

2 Methodology

2.1 Experimental Setup

The open jet facility available in the High-Speed Aerodynamics Laboratory, Department of Aerospace Engineering, SRMIST, Chennai, was utilized for the experimental study. The experimental setup was specifically designed and calibrated to study the effect of air tabs. The setup consisted of a storage tank, a ball valve, a pressure-regulating valve, a 1-meter-long mixing length, a primary settling chamber, and a slot holder. At the exit of the primary settling chamber, the convergent-divergent nozzle was secured using the slot holder. The pressurized air from the storage tank was delivered to the nozzle exit through the ball valve, pressure regulator, and primary settling chamber. The pressure inside the primary settling chamber (p_{0s}) was maintained with the help of a pressure-regulating valve. An injection settling chamber was used to deliver pressurized fluid to the air tabs for fluidic injection. A control valve was also used to regulate the pressure (p_{0i}) in the injection settling chamber. A pressure scanner was used to monitor the pressures in both chambers during the whole experiment. The temperature inside both chambers was

equivalent to the local atmospheric temperature. The illustrative representation of the experimental setup is depicted in Figure 1.

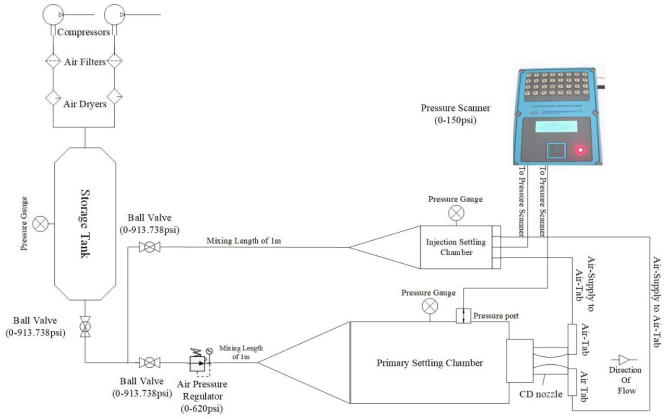

Fig 1. Schematic view of the experimental setup

The use of a convergent-divergent nozzle to generate a Mach 2.1 jet with sonic injection has not been studied previously. In the present study, a circular convergent-divergent nozzle was calibrated to ensure it delivers a supersonic jet of Mach number 2.1. The diameter of the nozzle throat (D_{th}) was 9.6 mm and the nozzle exit diameter (D) was 13.00 mm. The "isentropic nozzle pressure ratio" (NPR) for the correctly expanded nozzle was found to be 9.14. The nozzle calibration was done using various mainstream actual total pressure values (p_{0s}) to produce a Mach 2.1 jet. At various NPRs, the distribution of the pitot pressure values along the diameter of the nozzle outlet was calculated. The total pressure at the probe nose downstream of the detached shock is indicated by the pitot pressure (p_{0t}). The measured p_{0t} was used in conjunction with "normal shock relation", as shown in equation (1)[10] to get the Mach number of the fluid flow. The value of p_{0s} is the total pressure of the main jet and it can be assumed to be equal to the settling chamber pressure as the flow through the nozzle can be considered as isentropic.

$$\frac{p_{0t}}{p_{0s}} = \left(\left(1 + \frac{2\gamma}{\gamma+1} \left(M_e^2 - 1 \right) \right)^{\left(-\frac{1}{\gamma-1} \right)} \times \left(\frac{(\gamma+1)M_e^2}{(\gamma-1)M_e^2+2} \right)^{\left(\frac{\gamma}{\gamma-1} \right)} \right) \tag{1}$$

The air tabs used in the experiments consisted of two constant area tubes with a 0.1 mm thickness and 1 mm inner diameter. The air tabs were positioned along the Y-axis, opposite to each other at the nozzle exit, as shown in Figure 2 a. The air tabs are placed 2 mm apart from the nozzle exit's circumference to prevent interference with the primary jet. The experimental setup of the circular nozzle with the air tabs is depicted in Figure 2 b.

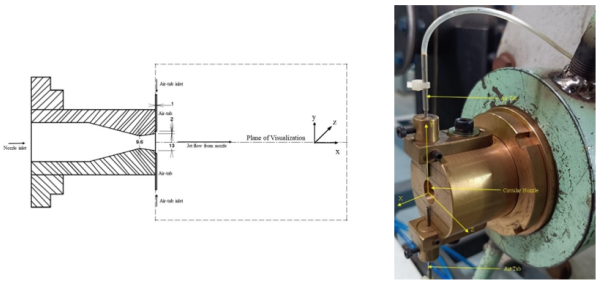

(a) (b)

Fig 2. (a) Side-view of the nozzle with air tabs at the exit and (b) experimental setup of air tabs at nozzle exit (all dimensions in mm)

- **Instrumentation**

The pressure measurements in the jet flow field were carried out using the pitot probe (thickness of 0.1mm; inner diameter of 0.8mm) connected to the pressure scanner. The probe was fixed to a traverse mechanism having a linear translation resolution of 0.1 mm. The traversing mechanism was used for the pressure measurements along all three axes. The blockage effect caused by the pitot probe is considered insignificant when the nozzle exit area to the pitot probe area ratio exceeds 64. In this study, the ratio was found to be 169, which is greater than the threshold value of 64.

The pressure scanner used in the present study has a range of 0 - 10.34 bar, a response time of 1 ms, and a sampling frequency of 100 Hz. Each recorded pressure reading represents a mean of 100 samples. To obtain a single pressure reading for a given position, the mean of the 100 readings is to be calculated. To visualize the jet waves, the shadowgraph technique was employed. The technique involves using a light source, a parabolic mirror (diameter of 200 mm and a focal length of 2.2 m), and a high-resolution camera (DSLR) for capturing shadowgraph images.

3 Results and Discussion

In this study, the total pressure behind the detached shock is represented as the pressure measurement. To determine the actual total pressure, it is essential to consider the pressure loss caused by the shock. However, correcting the measured pitot pressure for the shock-induced losses proves challenging due to variations in Mach number within the core and the varying strength of shock waves in different shock cells. Consequently, obtaining precise values for the actual total pressure becomes difficult. Therefore, it is crucial to interpret the findings of the supersonic jet flow field as qualitative rather than quantitative. While they may not provide precise numerical values, the results are still valuable for comparative purposes. They allow for meaningful comparisons between different cases or scenarios under investigation, enabling a qualitative assessment of the impact of the introduced air tabs on the jet flow field.

3.1 Centerline Pressure Decay

The pitot pressure measurements along the jet centerline were used to quantify the jet core length and different zones of characteristic decay within the jet region. Pressure measurements were noted at intervals of 1 mm along the jet axis, up to 20 times the nozzle exit diameter (i.e. 20D). The centerline pressure decay plot indicates the degree of mixing between the jet flow and the surrounding environment. The analysis of the centerline pressure decay plot helps to estimate the length of the supersonic core. Unlike subsonic flow, the supersonic flow contains waves in the jet core region. These waves induce pitot pressure oscillations resulting in non-uniform velocity in the jet core. Even in a correctly expanded jet, these waves are caused by the relaxation effect [7].

The effect of air tabs on jet mixing was evaluated using the data obtained from pitot pressure (p_{0t}) measurements along the centerline of the jet normalized with respect to the stagnation pressure (p_{0s}). The axial distance from the exit of the nozzle (X) was normalized with respect to the nozzle exit diameter (D). The pitot pressure measurements of both the controlled jet (with an air tab) placed at the nozzle exit (0D) and the uncontrolled jet were plotted for various IPRs of 3, 4, 5, and 6 while maintaining fixed NPRs of 3, 4, 5, and 6 corresponding to overexpanded states for Mach 2.1 jet.

Figure 3 a present the centerline pressure decay plot for NPR 3. In the highly over expanded condition, the core length values for IPRs of 3, 4, 5, and 6 were determined to be 2D, 1.54D, 1.31D, and 0.31D, respectively. Comparatively, the uncontrolled jet exhibited a core length of 2.23D. The percentage reduction in core length for IPRs 3, 4, 5, and 6 amounted to 10.3%, 30.9%, 41.3%, and 86.1%, respectively. Notably, the core length reduction increased with higher IPR values, and the controlled jet showcased shorter pressure oscillations in the near field. The highest core length reduction of 86.1% was observed at IPR 6, emphasizing significant jet mixing characteristics.

Similarly, for NPR 4, the centerline pressure decay plot represented in Figure 3 b shows that under highly over expanded conditions, the core length values for IPRs 3, 4, 5, and 6 were 2.46D, 2.31D, 2.15D, and 2.0D, respectively. While the core length of the uncontrolled jet was 5.69D. The percentage reduction in core length for IPRs 3, 4, 5, and 6 reached 56.8%, 59.4%, 62.2%, and 64.9%, respectively. With an increase in the IPR significant reduction in the core length was observed. Also, there was a noticeable increase in pressure oscillations in the near field when moving from NPR 3 to 4. The core length reduction was maximum at IPR 6 with 64.9%.

Figure 3 c exhibits the centerline pressure decay plot for NPR 5, where the jet is in an over expanded condition. The core length values for IPRs 3, 4, 5, and 6 were found to be 5.46D, 4.31D, 4.08D, and 2.76D, respectively. The uncontrolled jet displayed a core length of 7.10D. The percentage reduction in core length for IPRs 3, 4, 5, and 6 amounted to 23.1%, 39.3%, 42.5%, and 61.1%, respectively. As with previous cases, higher IPR values yielded increased core length reduction, and there was a pronounced

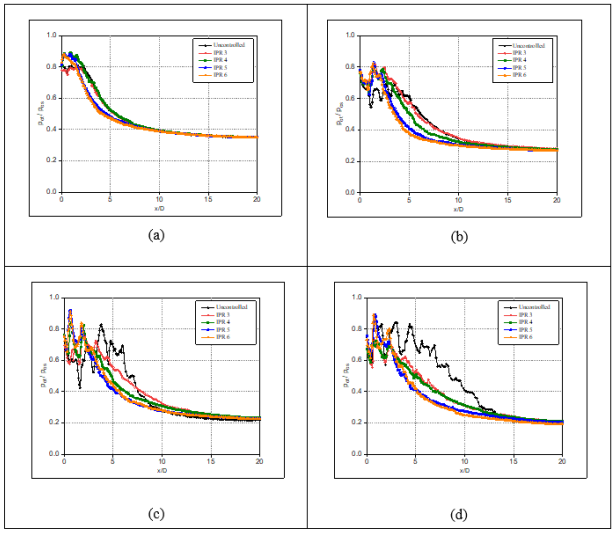

Fig 3. Centerline pitot pressure decay of uncontrolled and controlled jets for varying IPRs at; (a) NPR 3, (b) NPR 4, (c) NPR 5, (d) NPR 6.

increase in pressure oscillations in the near field as NPR increased from 4 to 5. The maximum core length reduction of 61.1% was observed at IPR 6.

Figure 3 d showcases the centerline pressure decay plot for NPR 6, where the jet is in an over expanded condition. The core length values for IPRs 3, 4, 5, and 6 were determined to be 6.31D, 5.40D, 5.0D, and 4.69D, respectively. The uncontrolled jet exhibited a core length of 10.76D. The percentage reduction in core length for IPRs 3, 4, 5, and 6 reached 41.4%, 49.8%, 53.5%, and 56.4%, respectively. As observed previously, increasing IPR values led to greater core length reduction, and there was an evident increase in pressure oscillations in the near field as NPR increased from 5 to 6. The maximum core length reduction of 56.4% was observed at IPR 6.

From Figure 3 a-d, it can be inferred that, for a fixed NPR, an increase in IPR results in a higher percentage reduction in core length. The reduction in core length can be attributed to the increased momentum of fluid injected by the air tab, which enhances mixing by generating stream wise vorticity in the main jet and altering the downstream shock cell structure. This mixing promotion weakens shock waves in the near field of the jet.

Similar to the present findings, in a previous study on the effect of steady fluidic injection in Mach 2 jet control using empirical scaling analysis, Arun Kumar et al.[8] observed a significant reduction in core length with an increase in the mass flow ratio of the mini jet to the main jet. Additionally, a reduction in core length and enhanced mixing was caused by the fluidic injection. Also, Kumar et al.[11] have reported that by introducing air tabs at the nozzle exit, the potential core length of the controlled jets could be reduced in Mach 0.6 jets. In Mach 2.0 elliptic jet with truncated triangular tabs, the mixing promotion was observed to be better than circular nozzles, wherein the core length reduction was observed to be increasing with the increase in NPR till the correctly expanded state, while it decreased in the under expanded condition[10]. These results from previous studies are in agreement with the present findings, which substantiate the effectiveness of utilizing sonic air tabs in Mach 2.1 jets for efficient jet mixing and enhancement.

3.2 Core length Variation with Injection Pressure Ratio

Figure 4 shows a plot between the non-dimensionalized core length (Lc/D) and the nozzle pressure ratio (NPR). As evident from the figure, the core length increases as NPR increases for both controlled and uncontrolled jets. However, when comparing the core lengths of both controlled and uncontrolled jets, the uncontrolled jet consistently exhibited the highest core length for NPRs 3, 4,5, and 6. The shortest core length was observed in the controlled jet with an IPR of 6.

For NPR 3, the core lengths of the uncontrolled jet and controlled jets with IPRs 3, 4, 5, and 6 were 2.23, 2, 1.54, 1.31, and 0.31, respectively. At NPR 4, the core lengths for the uncontrolled jet and controlled jets with IPRs 3, 4, 5, and 6 were 5.69, 2.46, 2.31, 2.15, and 2.00, respectively. The core lengths for NPR 5 were 7.1, 5.46, 4.31, 4.08, and 2.76 for the uncontrolled jet and controlled jets with IPRs 3, 4, 5, and 6. Finally, for NPR 6, the core lengths for the uncontrolled jet and controlled jets with IPRs 3, 4, 5, and 6 were 10.76, 6.31, 5.40, 5.00, and 4.69, respectively.

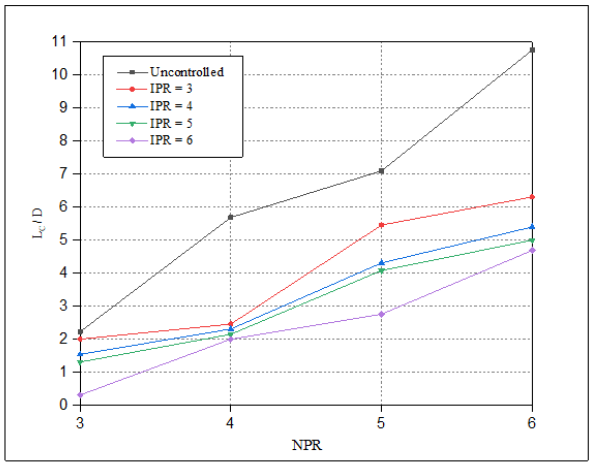

Fig 4. Core length variation of uncontrolled and controlled jets with NPR at different IPRs

The graph indicates that an increase in IPR leads to a reduction in core length for a fixed NPR. This reduction can be attributed to the increased momentum injection by the air tab as IPR increases, promoting mixing by generating streamwise vorticity in the main jet and altering the structure of downstream shock cells. This enhanced mixing weakens shock waves in the near field of the jet. Additionally, an increase in NPR results in an increased core length due to greater momentum in the primary jet.

In a previous study using Mach 2.0 jet controlled using rectangular tabs, three forms of flow categories were detected i.e., the "jet bifurcation", "complex and strong shock-cell structure" and "weak shock structure". Placing the tab behind the first shock cross-over point resulted in a shorter core length and increased jet mixing [(3)]. In a convergent-divergent nozzle delivering Mach 1.8, the positioning of two short rectangular vortex-generating actuators, diametrically opposite to each other, led to a significant 75% reduction in the core length for NPR 5. Additionally, the controlled jet exhibited an increase in jet spread downstream of the nozzle exit when compared to the uncontrolled jet at NPRs 4, 5, 6, 7, and 8 [(12)]. The present research findings are in significant agreement with the previous literature. The consistency between the results of previous studies and the current findings shows that using sonic air tabs in Mach 2.1 jets can indeed be effective for achieving efficient jet mixing and enhancement.

3.3 Radial Profiles of Pitot Pressure Measurements

Measuring the pitot pressure variation along the y-direction and z-direction can provide insights into the effects of control on jet symmetry and mixing. By measuring the pitot pressure distribution along the z-direction the jet's axial symmetry can be evaluated. An ideally symmetric jet would exhibit a uniform pitot pressure variation along the z-axis. However, if there is an asymmetry in the control, it may cause variations in the pitot pressure distribution, indicating deviations from axial symmetry. Pitot pressure measurements provide insights into the radial distribution of pitot pressure and illustrate the changes in flow behavior as the distance from the nozzle exit increases. The study involved measuring the pitot pressure distribution along the z-axis at various locations (x/D = 0, 1, 2, 4, 8, and 16) for different IPR values, namely 3, 4, 5, and 6. These measurements were conducted for corresponding NPRs of 3, 4, 5, and 6 as well.

The pitot pressure distribution along the z-axis at different locations (x/D = 0, 1, 2, 4, 8, and 16) for IPRs 3, 4, 5, and 6, with a corresponding NPR of 3, 4, 5 and 6 were recorded. The presence of shock waves in the near field of the jet was evident. These shock waves signify abrupt changes in pressure and flow characteristics that significantly affect the jet's behavior. Progressing downstream along the jet axis, the influence of jet mixing becomes more apparent. The jet undergoes mixing with the surrounding medium, resulting in spreading and dispersion over a larger area. Notably, IPR 6 exhibited accelerated mixing and a reduction in the jet's core length. This indicated that IPR 6 enhances the efficiency of jet mixing with the surrounding medium, leading to a shorter core length.

In Figure 5, the distribution of pitot pressure along the z-axis at various locations along the x-axis for IPRs 3, 4, 5, and 6, corresponding to a fixed NPR of 4 was illustrated. In Figure 5 (a), (b), (c), and (d), shock waves persisted until x/D = 4, consistent with the pressure decay observed along the centerline. Similarly, Figure 6 displays the pitot pressure distribution along the z-axis at various locations for IPRs 3, 4, 5, and 6, with a corresponding NPR of 6. The plot clearly shows that shock waves are more

pronounced in the uncontrolled jet compared to the controlled jet. In Figure 6 (a), (b), (c), and (d) the shock waves can be seen. As x/D was increased, IPR 6 exhibited a significant pressure drop compared to the uncontrolled jet and the other IPRs of the controlled jet. Furthermore, the shock strength decreases with an increase in IPR. Consistent with lower NPRs, an increase in the distance along the jet axis leads to noticeable jet spread, accompanied by a substantial drop in pressure, indicating effective jet mixing due to the introduction of an air tab.

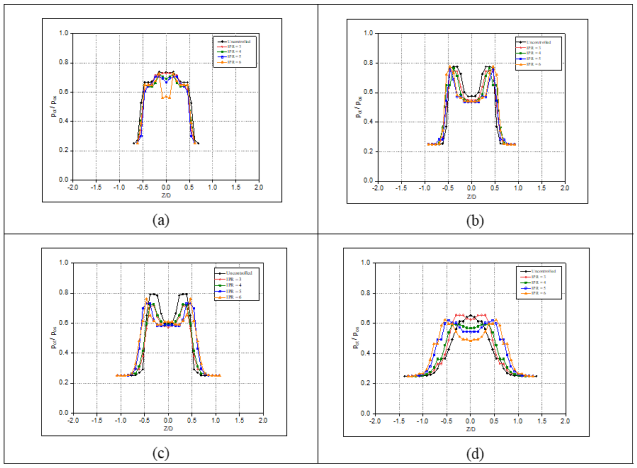

Fig 5. Radial pitot pressure profiles for uncontrolled and controlled jets at NPR 4; (a) x/D = 0, (b) x/D = 1, (c) x/D = 2, (d) x/D = 4.

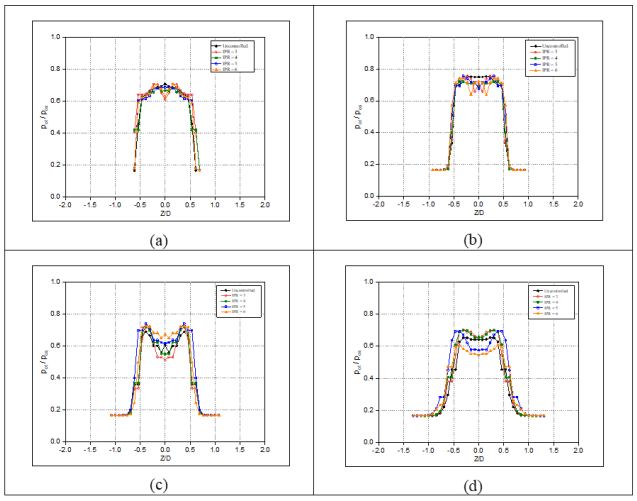

Fig 6. Radialpitot pressure profiles for uncontrolled and controlled jets at NPR 6; (a) x/D= 0, (b) x/D = 1, (c) x/D = 2, (d) x/D = 4.

In summary, the radial pitot pressure plots demonstrate that as the IPR increases, there is a corresponding significant increase in the pressure drop within the jet. This indicated that higher IPR values lead to more pronounced pressure variations, highlighting the enhanced mixing of the injected flow with the primary flow. Additionally, as the NPR increases from 3 to 6, there is a notable and substantial increase in the pressure drop. The results signified that higher NPR values result in more effective jet mixing. The increased pressure drop suggests that the injected flow interacts more vigorously with the surrounding medium, leading to enhanced jet spreading and dispersion. This phenomenon indicates a higher degree of mixing between the jet and its environment.

Similar to the present study, in a Mach 2.0 round jet the mixing enhancement using two steady radial injectors was found to be more efficient than an elliptic jet, hence it was suggested that fluidic injectors or air tabs are more effective and flexible in jet

operations [13]. In a rectangular sonic jet, fluidic injection using air tabs at the nozzle exit along the minor axis promoted mixing and core length reduction at all NPRs and the mixing increased with increasing IPRs [14]. In a Mach 1.8 supersonic jet generated with a convergent-divergent nozzle, the use of two short rectangular vortex-generating actuators located diametrically opposite to each other, resulted in a 75% core length reduction compared to the uncontrolled jet for NPR 5 [12].

3.4 Flow Visualization

The results of shadowgraph visualization of controlled and uncontrolled jets were compared to analyze the effect of sonic air tabs on the shock structure of Mach 2.1 jet. The visualization results confirmed the findings from the centerline pressure measurements, particularly the observation of core length reduction caused by the presence of air tabs. The results also show that with increasing IPR, the reduction is more pronounced for a given NPR. Thus, the visualization results support the findings made from the centerline and radial profile plots. Representative shadowgraph results at NPRs 5 and 6 for varying IPRs supporting the above discussion are presented in Figure 7 . Figure 7 (a) and (f), correspond to shadowgraph images of the uncontrolled jet at NPR 5 and NPR 6. Figure 7 (b) to (e) and (g) to (j) represent the results of the controlled jet at NPR 5 and NPR 6 for IPRs 3 to 6 respectively. Another important aspect to be noticed from the results is that the air tabs are effective in rendering the waves weaker in the jet core. This is evident from the decrease in the intensity of waves with increasing IPR (Figure 7). The reduced wave strength in the jet core with increasing IPR is due to the increased mixing promotion caused by air tabs. The weakening of waves by air tabs offers an advantage from an aero-acoustic perspective.

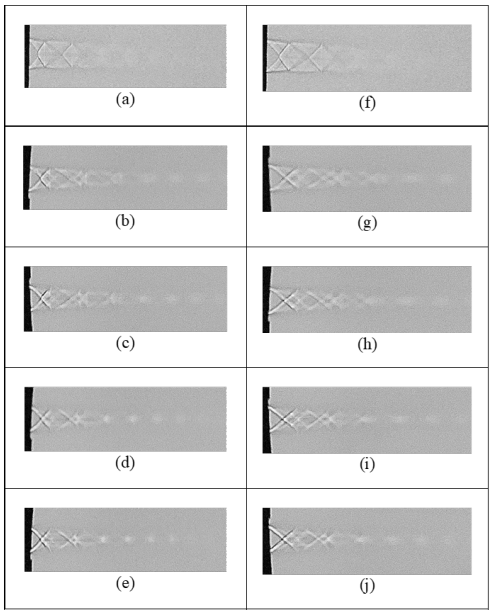

Fig 7. Shadow graph images of uncontrolled and controlled jets at NPRs 5 and 6 for varying IPRs; (a) Uncontrolled jet at NPR5, (b) Jet with IPR 3 at NPR 5, (c) Jet with IPR 4 at NPR 5, (d) Jet with IPR 5at NPR 5, (e) Jet with IPR 6 at NPR 5, (f) Uncontrolled jet at NPR 6, (g) Jet with IPR 3 at NPR 6, (h) Jet with IPR 4 at NPR 6, (i) Jet with IPR 5 at NPR 6,(j) Jet with IPR 6 at NPR 6.

In summary, the air tabs are effective in mixing the promotion of Mach 2.1 jet as evident from the shadow graph images of the uncontrolled and controlled jets. The air tabs are also proved to be advantageous from the aero-acoustic point of view as they render the waves weaker in the jet core. In a previous study, according to Kailash et al. [15], in the case of a sonic rectangular jet, an increase in the injection pressure ratio (IPR) of sonic air tabs led to a reduction in core length for the minor axis injection, while the opposite trend was observed for the major axis injection at each nozzle pressure ratio (NPR). They also reported that the presence of air tabs resulted in the weakening of waves due to shock waves from the injected sonic air tab. In general, the introduction of fluidic injection or air tab into the Mach 2.1 main jet generated counter-rotating vortex pairs (CVPs), which moved toward the main jet axis with their velocity. When the CVPs are close enough their velocity becomes stronger and distorts the main jet. The distortion of the main jet forms longitudinal vortices moving along the streamwise direction and entraining the surrounding ambient fluid into the jet core thereby enhancing jet mixing.

3.5. Comparative analysis of the present study with the literature

Figure 8 illustrates a comparative plot highlighting the findings of the current study in relation to the research conducted by Jabez Richards et al.[14] wherein, they employed two rectangular tabs featuring isosceles triangular projections on each tab. These tabs were strategically positioned diametrically opposite at the nozzle exit. The study focused on a convergent nozzle with an exit Mach Number of 0.8. Notably, the introduction of these tabs led to a reduction in the potential core length from 6.5D to 1.25D. Remarkably, our current study observed a similar trend while studying the control of a circular jet with a Mach Number of 2.1. In this scenario, an air tab placed at the nozzle exit, with an Injection Pressure Ratio (IPR) and Nozzle Pressure Ratio (NPR) both set to 3, was employed. This air tab caused a reduction in the potential core length from 2.2 D to 2D

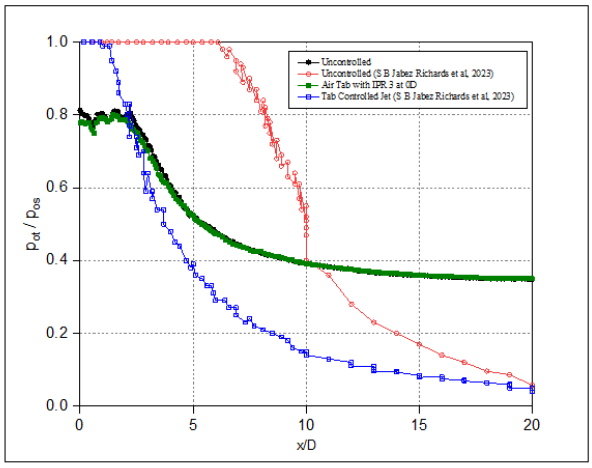

Fig 8. Comparative plots of centerline pitot pressure decay of uncontrolled and controlled jets with S. B. Jabez Richards et al.[14] .

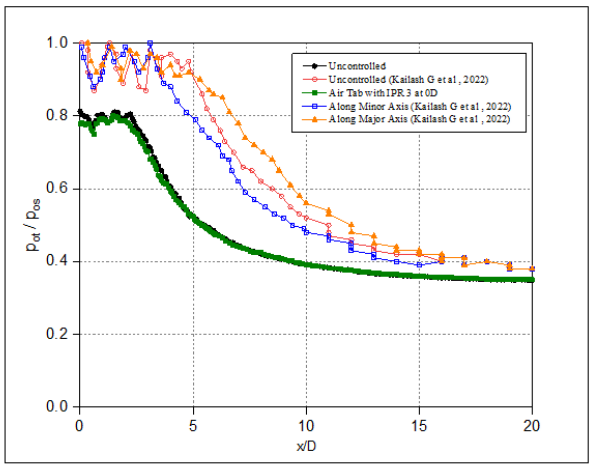

Fig 9. Comparative plots of centerline pitot pressure decay of uncontrolled and controlled jets with Kailash G et al.[15]

In Figure 9 , a comparative plot is depicted, showcasing the outcomes of our study in comparison to the research conducted by Kailash et al.[15] . In their investigation, they studied a rectangular sonic jet with an aspect ratio of 2. They employed sonic fluidic injection through two air tabs positioned diametrically opposite to each other along both the minor and major axes of the nozzle exit. By introducing an air tab along the minor axis with NPR 3 and IPR 3, the potential core length was reduced from 4.8D to 3D. Conversely, the introduction of air tabs along the major axis led to an increase in the potential core length

from 4.8D to 6D. Interestingly, in our study, when employing an air tab at the nozzle exit with IPR 3 and NPR 3 for controlling a circular jet at Mach 2.1, the potential core length decreased from 2.2D to 2D. These results align with the findings of the air tab orientation along the minor axis but deviate from those of the air tab orientation along the major axis.

4 Conclusion

In conclusion, this study introduces a novel approach by implementing sonic air tabs at the nozzle exit to enhance the mixing efficiency of a Mach 2.1 jet. The core length of the Mach 2.1 jet consistently decreases as the Injection Pressure Ratio (IPR) increases for the investigated NPRs of 3, 4, 5, and 6. The percentage reduction in core length becomes more pronounced as the IPRs increase for all NPRs, primarily due to the increased momentum injection facilitated by the air tab. This augmented momentum injection generates streamwise vorticity within the main jet and modifies the downstream shock structure, resulting in enhanced mixing. As a result of this mixing promotion, the strength of shock waves in the vicinity of the jet's exit is mitigated. For NPR 3, the percentage reduction in core length for IPRs 3, 4, 5, and 6 ranges from 10.3% to 86.1%. For NPR 4, the percentage reduction in core length varies from 56.8% to 64.9%. Similarly, for NPR 5, the percentage reduction in core length ranges from 23.1% to 61.1%. For NPR 6, the percentage reduction in core length varies from 41.4% to 56.4%. These results clearly show the significant impact of sonic air tabs in enhancing mixing and reducing the core length of Mach 2.1 jet, particularly at higher IPRs.

The findings of this study contribute to the understanding of fluidic control techniques and their potential applications in improving jet mixing and noise reduction. The current investigation shows the intricate relationship between the momentum injection facilitated by the air tab and its effects on shock structure modification and improved jet mixing. Based on the findings, it is recommended to consider the integration of sonic air tabs as a viable strategy for enhancing mixing in Mach 2.1 jet engines. Future research prospects include optimizing the design parameters of sonic air tabs and considering variables such as nozzle geometry, air tab placement, and different flow conditions.

Acknowledgement

We thank the technical support rendered by the technicians associated with the open jet facility in the High-Speed Aerodynamics Laboratory, Department of Aerospace Engineering, SRMIST, Chennai.

References

1) Das AK, Acharyya K, Mankodi TK, Saha UK. Fluidic Thrust Vector Control of Aerospace Vehicles: State-of-the-Art Review and Future Prospects. *Journal of Fluids Engineering*. 2023;145(8). Available from: https://doi.org/10.1115/1.4062109.
2) Khan A, Rao AN, Baghel T, Perumal AK, Kumar RK. Parametric study and scaling of Mach 1.5 jet manipulation using steady fluidic injection. *Physics of Fluids*. 2022;34(3). Available from: https://doi.org/10.1063/5.0078089.
3) Kumar PA, Aileni M, Rathakrishnan E. Impact of tab location relative to the nozzle exit on the shock structure of a supersonic jet. *Physics of Fluids*. 2019;31(7):76104. Available from: https://doi.org/10.1063/1.5111328.
4) Benderradji R, Gouidmi H, Beghidja AA. Effect of the fluidic injection on the flow of a converging-diverging conical nozzle. *International Journal of Energetica*. 2020;5(1):07. Available from: http://dx.doi.org/10.47238/ijeca.v5i1.114.
5) Kumar A, Kumar SMA, Mitra AS, Rathakrishnan E. Empirical scaling analysis of supersonic jet control using steady fluidic injection. *Physics of Fluids*. 2019;31(5):56107. Available from: https://doi.org/10.1063/1.5096389.
6) Semlitsch B, Cuppoletti DR, Gutmark EJ, Mihăescu M. Transforming the Shock Pattern of Supersonic Jets Using Fluidic Injection. *AIAA Journal*. 2019;57(5):1851–1861. Available from: https://dx.doi.org/10.47238/ijeca.v5i1.114.
7) Rathakrishnan E. Applied Gas Dynamics. vol. 656. Wiley. 2019. Available from: https://books.google.co.in/books?id=W1-HDwAAQBAJ.
8) Sekar C, Jaiswal K, Arora R, Sundararaj RH, Kushari A, Acharya A. Nozzle Performance Maps for Fluidic Thrust Vectoring. *Journal of Propulsion and Power*. 2021;37(2):314–339. Available from: https://doi.org/10.2514/1.B38044.
9) Thangaraj T, Kaushik M, Deb D, Unguresan M, Muresan V. Survey on Vortex Shedding Tabs as Supersonic Jet Control. *Frontiers in Physics*. 2022;9:789742. Available from: https://doi.org/10.3389/fphy.2021.789742.
10) Thomas J, Khurana S. Over-expanded Elliptical Jet Control using Truncated-Triangular Tabs. *AIAA SCITECH*. 2022. Available from: https://doi.org/10.2514/6.2022-1066.
11) Kumar N, Pannerselvam V, Thanigaiarasu S, Sinhamahapatra KP. Experimental and Numerical Investigation of Subsonic Free Jet Controlled by Air Tabs. *AIAA AVIATION* . 2023. Available from: https://doi.org/10.2514/6.2023-4435.
12) Ranjan A, Kaushik M, Deb D, Muresan V, Unguresan M. Assessment of Short Rectangular-Tab Actuation of Supersonic Jet Mixing. *Actuators*. 2020;9(3):72. Available from: https://doi.org/10.3390/act9030072.
13) Perumal AK, Rathakrishnan E. Design of Fluidic Injector for Supersonic Jet Manipulation. *AIAA Journal*. 2022;60(8):4639–4648. Available from: https://doi.org/10.2514/1.J061257.
14) Kailash G, Kumar SMA. Effect of Fluidic Injection on the Core Length of Rectangular Sonic Jet. In: Recent Advances in Applied Mechanics. Springer Singapore. 2022;p. 87–94. Available from: https://doi.org/10.1007/978-981-16-9539-1_6.
15) Kailash G, Kumar SMA. Control of sonic jets by fluidic injection. *IOP Conference Series: Materials Science and Engineering*. 2020;912(2):022012. Available from: https://doi.org/10.1088/1757-899X/912/2/022012.